Translational Oncology
www.transonc.com

Volume 6 Number 6 December 2013 pp. 638–648 638

Ionizing Radiation and Glioblastoma Exosomes: Implications in Tumor Biology and Cell Migration[1,2]

W. Tris Arscott*,†,‡, Anita T. Tandle*, Shuping Zhao*, Jacob E. Shabason*,‡,§, Ira K. Gordon*, Cody D. Schlaff*, Guofeng Zhang¶, Philip J. Tofilon* and Kevin A. Camphausen*

*Radiation Oncology Branch, National Cancer Institute, Bethesda, MD; †University of Vermont College of Medicine, Burlington, VT; ‡Howard Hughes Medical Institute–National Institutes of Health Research Scholars Program, Bethesda, MD; §Department of Radiation Oncology, University of Pennsylvania School of Medicine, Philadelphia, PA; ¶Biomedical Engineering and Physical Science Shared Resource, National Institute of Biomedical Imaging and Bioengineering, Bethesda, MD

Abstract

Exosomes are nanometer-sized lipid vesicles released ubiquitously by cells, which have been shown to have a normal physiological role, as well as influence the tumor microenvironment and aid metastasis. Recent studies highlight the ability of exosomes to convey tumor-suppressive and oncogenic mRNAs, microRNAs, and proteins to a receiving cell, subsequently activating downstream signaling pathways and influencing cellular phenotype. Here, we show that radiation increases the abundance of exosomes released by glioblastoma cells and normal astrocytes. Exosomes derived from irradiated cells enhanced the migration of recipient cells, and their molecular profiling revealed an abundance of molecules related to signaling pathways important for cell migration. In particular, connective tissue growth factor (CTGF) mRNA and insulin-like growth factor binding protein 2 (IGFBP2) protein levels were elevated, and coculture of nonirradiated cells with exosomes isolated from irradiated cells increased CTGF protein expression in the recipient cells. Additionally, these exosomes enhanced the activation of neurotrophic tyrosine kinase receptor type 1 (TrkA), focal adhesion kinase, Paxillin, and proto-oncogene tyrosine-protein kinase Src (Src) in recipient cells, molecules involved in cell migration. Collectively, our data suggest that radiation influences exosome abundance, specifically alters their molecular composition, and on uptake, promotes a migratory phenotype.

Translational Oncology (2013) 6, 638–648

Introduction

The microenvironment plays an important role in tumor progression and gene expression and influences response to therapeutic interventions [1,2]. Extracellular vesicles—including microvesicles and exosomes, herein referred to as exosomes—are nanometer-sized membrane-derived vesicles (averaging 100 nm in size) that contain various bioactive substances including RNA species [3], full-length protein receptors, ligands [4,5], and DNA [6]. Exosomes can be found in various bodily fluids and are secreted by cells in culture [7], and their composition is largely dependent on their cell of origin [8]. Tumor exosomes are thought to be an important mediator of intercellular signaling, fusing with recipient cells and transferring their bioactive molecules [3,7,8]. These events enable communication between different tumor cells and between tumor cells and the surrounding stromal cells. Specifically in cancer, this mode of intercellular signaling has been shown to promote angiogenesis [9,10], transfer oncogenes and tumor suppressor genes [5,11,12],

Address all correspondence to: Kevin A. Camphausen, Radiation Oncology Branch, National Cancer Institute, 10 Center Drive 3B42, Bethesda, MD 20892.
E-mail: camphauk@mail.nih.gov

[1]This research was supported in part by the Intramural Research Program of the National Institutes of Health, National Cancer Institute. No conflict of interest to disclose.
[2]This article refers to supplementary materials, which are designated by Figures W1 to W3 and are available online at www.transonc.com.
Received 25 September 2013; Revised 25 September 2013; Accepted 30 October 2013

DOI 10.1593/tlo.13640

enhance cell invasion [13], modulate the immune system [14], and help establish a premetastatic niche [10,11]. Moreover, given their small size and membrane protective coat, exosomes are capable of traveling throughout the body to influence cell function at distant sites [11] and are gaining attraction as novel clinical biomarkers [5,15,16].

Of the invasive cancers, glioblastoma multiforme (GBM) is considered one of the most aggressive and lethal. GBMs are capable of influencing their microenvironment driving angiogenesis, evading the immune system, and promoting degradation of the extracellular matrix leading to local invasion [17]. Their local invasiveness results in poorly defined margins for surgery, suboptimal treatment planning for radiation therapy, and their nearly universal recurrence in patients, with a median survival of 15 months [18]. Although numerous mechanisms contributing to the invasiveness of GBM have been found, further studies identifying targetable mechanisms are needed.

Exosomes, given their small size and vast influence on cells within the tumor and greater microenvironment, are an attractive target. Although hypoxia has been shown to influence exosome composition [19,20], there is, overall, a void of literature discussing how cancer therapies influence exosome-mediated intercellular signaling. Here, we provide evidence that radiation increases exosome release in a variety of GBM cell lines and normal astrocytes. Exosomes released from irradiated GBM cells enhanced the migration of recipient cells in comparison to exosomes derived from nonirradiated cells, which was abrogated by lysing exosomes before transferring them to cells. These exosomes had a molecular profile containing an abundance of molecules important for cell motility, in particular increased connective tissue growth factor (CTGF) mRNA and insulin-like growth factor binding protein 2 (IGFBP2) protein. Moreover, when exosomes from irradiated cells were taken up by nonirradiated cells, they increased the expression of CTGF protein, likely a result of translation of the exosome mRNA, as well as enhanced the activation of the signaling molecules involved in cell migration, including increased activation of neurotrophic tyrosine kinase receptor type 1 (TrkA), focal adhesion kinase (FAK), Paxillin, and proto-oncogene tyrosine-protein kinase Src (Src).

Materials and Methods

Cell Lines

LN18, U87MG [American Type Culture Collection (ATCC), Manassas, VA], and U251 (National Cancer Institute Frederick Tumor Repository, Frederick, MD) GBM cell lines were grown in Dulbecco's modified Eagle's medium (DMEM; Invitrogen, Carlsbad, CA) with 10% FBS, used between passages 4 to 16, and revived every 2 to 3 months from frozen stocks made after receiving cell lines. Cell lines were recently validated by Idexx Radil Laboratories (Columbia, MO). U87MG cells expressing green fluorescent protein (GFP) were graciously provided by Dr Jayne Stommel. GBAM1 and GBMJ1, GBM stem-like cells, were established from patient resections, grown as previously described [21], and used between passages 3 to 10. Astrocytes were purchased from ScienCell Research Laboratories (Carlsbad, CA), grown in Astrocyte Medium with the recommended supplements as per manufacturer's instructions, and used between passages 3 to 9. Human umbilical vein endothelial cells (HUVEC-CS) were obtained from ATCC, grown on gelatin-coated dishes in DMEM containing 20% FBS, as per manufacturer's instructions, and used up to passage 10. All cell cultures were maintained at 37°C and 5% CO_2/95% air, except stem cell cultures, which were maintained at 37°C and 5% CO_2/6% O_2.

Radiation Treatment

Cells at 70% to 80% confluency were washed twice with phosphate-buffered saline (PBS) and replenished with 5% exosome-depleted FBS (dFBS; see below) in DMEM (LN18, U251, and U87MG) or stem cell growth medium (GBAM1, GBMJ1, and astrocytes). Immediately following, the flasks were treated with the indicated radiation dose using an X-ray source (X-RAD 320; Precision X-Ray, North Branford, CT; dose rate, 2.3 Gy/min) and incubated for 12 to 48 hours before exosome isolation.

Exosome Isolation

Exosomes were isolated by ultracentrifugation, adapted from Théry et al. [22]. Cell media were clarified of cells and cellular debris by spinning media at 300*g* for 5 minutes, then at 3000*g* for 15 minutes at 4°C, before pelleting at 110,000*g* for 2 hours at 4°C. Exosomes were washed in PBS and repelleted by an additional spinning at 110,000*g* for 2 hours. Exosomes were resuspended in PBS or lysed in the appropriate buffer for additional analysis and stored at −20°C. Uncentrifuged complete media (CM) and supernatant from the first exosome pellet after ultracentrifugation were set aside for control experiments. dFBS was generated by spinning FBS at 110,000*g* for 16 hours at 4°C. The supernatant of this spin was used as dFBS.

Nanoparticle Tracking Analysis

Exosomes were analyzed for size and concentration using a NanoSight LM10 microscope and Nanoparticle Tracking Analysis software version 2.2 (NanoSight, Amesbury, United Kingdom). See [23] for details on application of the Nanoparticle Tracking Analysis (NTA) instrument for exosome analysis. Exosome samples were diluted to ~80 to 125 particles per frame for tracking, and >500 particles were tracked. Particle tracking time, exposure level, and analysis settings (detection threshold, auto; blur, 5 × 5; minimum size, 50 nm; minimum track length, default) were kept identical for each group of experiments, and each sample was analyzed twice to ensure accurate measurement.

Electron Microscopy

Scanning electron microscopy (EM) was carried out by the National Cancer Institute–Frederick Core facility (Frederick, MD). Transmission EM was performed by placing 5 μl of exosomes suspended in PBS on glow discharge copper grids and allowing them to settle for 1 minute before rinsing with distilled water. Exosomes were stained with 1% uranyl acetate for 15 seconds before letting the grids dry. Exosomes were examined under an FEI Tecnai12 transmission electron microscope (FEI, Hillsboro, OR) operating at a beam energy of 120 keV. Images were acquired using a Gatan 2k × 2k cooled charge-coupled device (CCD) camera (Gatan, Warrendale, PA).

Fluorescent Labeling of Exosomes

Exosomes were labeled with the red-fluorescing, lipophilic dye PKH26 according to the manufacturer's recommendations (Sigma, St Louis, MO) and Khatua et al. [24]. An equal volume of 5% dFBS/DMEM was used to stop labeling before repelleting and washing twice with 5% dFBS/DMEM to remove excess PKH26. Labeled exosomes were resuspended in PBS and stored at −20°C.

5-Bromouridine 5′-Triphosphate Labeling of Exosome RNA

Cells were grown in 5% dFBS media containing 100 μM 5-Bromouridine 5′-triphosphate (BrUTP, Sigma), following methods described by

Ohtsu et al. [25] to label nascent RNA. After 48 hours, media were collected; exosomes containing brominated mRNA were pelleted by ultracentrifugation. The exosomes containing brominated mRNA (25 μg/ml) were added in coculture with U87MG cells for 6 hours, after which cells were washed twice with PBS and fixed with normal buffered formalin, and a fluorescein isothiocyanate–conjugated anti-bromodeoxyuridine antibody (Santa Cruz Biotechnology, Dallas, TX; 1:50 dilution) was used to detect brominated RNA. Images were collected using a Leica upright fluorescent microscope (Leica, Solms, Germany).

Exosome Transfer Experiments

In a method guided by Al-Nedawi et al. [4], 15,000 cells were seeded on glass coverslips, allowed to adhere overnight, and washed twice with PBS, and then PKH26-labeled exosomes diluted 5 to 10 μg/ml in 5% dFBS/DMEM were added. At the indicated time point, coverslips were removed, washed once with PBS, fixed with 10% normal buffered formalin, washed twice in PBS, and mounted to slides with mounting medium containing 4′,6-diamidino-2-phenylindole (DAPI; Vector Shield, Burlingame, CA). Images were captured using a Carl Zeiss (Baltimore, MD) LSM 510 laser scanning confocal microscope. For flow cytometry, 100,000 cells were seeded into 12-well plates, allowed to adhere overnight, and then incubated with PKH26-labeled exosomes diluted 5 to 10 μg/ml in 5% dFBS/DMEM from 30 minutes to 24 hours. Measurement of uptake was captured using a FACSCalibur flow cytometer (BD Biosciences, Bedford, MA) and analyzed using FlowJo Software version 7.6.5 (Ashland, OR).

In vitro *Migration Assay*

Transwell chambers (BD Biosciences) were used for *in vitro* assays of cell migration according to the manufacturer's recommendation (pore size, 8.0 μm). Exosomes (isolated from culture media at 48 hours after treatment with 4 Gy or no irradiation) were diluted in serum-free DMEM in the lower chamber from 1 to 100 μg/ml. Cells were allowed to migrate for 24 hours; then the upper chamber was scraped twice to remove nonmigrated cells and stained with crystal violet, and the number of migrated cells was counted. Ten 20× fields were counted per condition using a Leica microscope. For pretreatment of cells with exosomes, cells were plated onto 100-mm dishes, incubated with 25-μg/ml exosomes for 24 hours, and then washed and seeded in serum-free DMEM in the upper chamber with no exosomes added to the lower chamber. For inhibition of migration experiments, exosomes or dFBS were incubated with 0.2% Triton X-100 (Tx-100) in PBS, at 37°C for 15 minutes before use.

Immunoblot analysis

Cells were seeded onto 60-mm dishes, allowed to attach overnight, washed twice with serum-free DMEM, and serum starved for 16 hours after which exosomes were added at a concentration of 25 μg/ml in serum-free DMEM. At 24 hours, cells were lysed in radioimmunoprecipitation assay (RIPA) buffer (Sigma) containing phosphatase (Sigma) and protease inhibitors (Roche, Indianapolis, IN). Protein concentration was quantified using a *DC* Protein Assay kit (Bio-Rad Laboratories, Hercules, CA). Thirty micrograms of protein was resolved on 4% to 20% Tris-Glycine gels and transferred to nitrocellulose membranes (Bio-Rad Laboratories). Immunoblot analysis of exosome lysates was done in the same fashion. Primary antibodies were given as follows: actin, CD9 (Millipore, Germany), CTGF, tumor susceptibility gene 101 (tsg101; Santa Cruz Biotechnology), apoptosis-linked gene 2-interacting protein X (Alix), IGFBP2, phospho-/total TrkA, phospho-/total FAK, phospho-/total Paxillin, and phospho-/total Src (Cell Signaling Technology, Danvers, MA). Secondary HRP-conjugated antibodies were purchased from Santa Cruz Biotechnology. Blots with exosome lysates or phosphorylated targets were developed using Super-Signal West Femto luminol substrate (Thermo Scientific, Rockfold, IL) and with other probes using ECL Prime luminol reagent (GE Healthcare, Pittsburgh, PA). Actin was used as a loading control.

Antibody Array Analysis

Pelleted exosomes were lysed as above. Glass protein arrays (human angiogenesis antibody array AAH-ANG-G1 and cytokine antibody array G series AAH-CYT-G6/7/8; RayBiotech, Norcross, GA) were used to detect protein levels in exosome samples. Assays were carried out according to the manufacturer's recommendations (15 μg of exosome lysate per subarray). Array values were standardized against the positive control within each subarray. Samples were run as biologic replicates, and a 1.33-fold change or greater was used as a cutoff to explore significant targets (increased or decreased abundance), comparing radiation-derived exosomes to those derived from nonirradiated cells.

Microarray Analysis for mRNA and microRNA

To characterize exosome RNA composition, total RNA was extracted from washed/pelleted exosomes using the *mir*Vana miRNA Isolation Kit (Invitrogen/Ambion) according to the manufacturer's recommendations. mRNA expression was assayed using cDNA arrays as previously described [26]. MicroRNA (miRNA) expression changes were analyzed using the FlashTag Biotin HSR RNA Labeling Kits and GeneChip miRNA 2.0 Arrays, according to the manufacturer's instructions (Affymetrix, Santa Clara, CA). R software was used to process cDNA array data by subsetting on the basis of P value of <.05 between conditions before further downstream analysis. A $\geq$1.33-fold change was used as a cutoff to explore significant increased/decreased targets comparing radiation-derived exosomes to those derived from nonirradiated cells for mRNA changes. The P value of <.05 was used as the only cutoff for the miRNA changes.

Real-Time Quantitative Polymerase Chain Reaction

Real-time quantitative polymerase chain reaction (PCR) was done using QuantiTect Reverse Transcription and SYBR Green PCR kits according to manufacturer's specifications (Qiagen, Valencia, CA). The following prevalidated primer sets were used: CTGF (Sigma) and beta-actin (ACTB) (Quanta BioSciences, Gaithersburg, MD). Reactions were run in an Applied Biosystems (Foster City, CA) 7500 Real-Time PCR thermal cycler, and the $2^{-\Delta\Delta Ct}$ method was used to calculate relative expression. ACTB was used as the endogenous control.

Ingenuity Pathway Analysis

Array data were analyzed using Ingenuity Pathway Analysis (IPA) software (Ingenuity Systems, Redwood City, CA) and a 1.33-fold cutoff for increased/decreased molecules to perform functional classifications comparing radiation-derived exosomes to those derived from nonirradiated cells. Top associated network functions and molecular/cellular functions were explored. Analyses were performed in the Spring 2012 build of IPA.

Statistical Analysis

All experiments were performed a minimum of three times, unless otherwise noted. Figures represent the average of independent replicates with the SEM. Statistical tests were two sided for comparisons between groups using a Student's *t* test. Comparison of dose enhancement in exosome abundance was analyzed using a one-way analysis of variance. A *P* value of <.05 was considered significant. All analyses were completed using R statistical software and GraphPad Prism (GraphPad Prism Inc, San Diego, CA).

Results

Confirmation of Exosome Isolation by Ultracentrifugation

The isolation of pure and intact exosomes was confirmed by scanning and transmission EM. Scanning EM showed budding vesicle–like structures on the surface of U87MG cells, which had a diameter of ~100 nm (Figure 1*A*). Transmission EM of U87MG exosomes showed characteristic disk-like exosomes, also ~100 nm in diameter (Figure 1*B*). NTA measured exosomes with a mean size of 139.83 ± 29.03 nm (SEM), which was not significantly influenced by irradiation (Figure W1*A*). Given the size distribution of the isolated exosomes in this work, the exosome preparation is likely devoid of apoptotic bodies that are larger [27], and irradiation of cells with 4 Gy does not induce significant apoptosis after a single fraction at 48 hours post-treatment [28,29]. To confirm that exosomes could be transferred to a recipient cell, PKH26-labeled exosomes were incubated with U87MG cells expressing GFP, and the labeled exosomes were visible within the cell cytoplasm confirming uptake by the cell, as well as along the cell's surface (Figure 1*C*). Immunoblot analysis showed that U87MG exosomes had known exosome markers [30]—Alix, tsg101, and CD9 (Figure 1*D*). A Ponceau stain of the nitrocellulose membrane demonstrated that exosomes contain a selective pool of proteins compared to the cells from which they were derived (Figure W1*B*).

Radiation Increases Exosome Release from Glioma and Nonglioma Cells

To examine the influence of radiation on exosome release, cells were grown in dFBS media, and exosomes were isolated from culture media 12 to 48 hours after irradiation. In irradiated LN18, U251, and U87MG cell lines, the increase in exosome abundance in culture media at 48 hours varied from 1.23- to 1.79-fold compared to the release of exosomes from nonirradiated controls (Figure 2*A*). GBM stem-like cells (GBAM1 and GBMJ1) showed increased release of exosomes following irradiation, with GBAM1 having a larger increase (2.6-fold; Figure 2*A*). We also observed an increase in exosomes released by normal astrocytes following irradiation (1.71-fold; Figure 2*A*).

We further characterized exosome release in U87MG and for subsequent molecular and functional studies. Irradiation of U87MG cells with 2 to 8 Gy significantly increased exosome abundance in a dose-dependent fashion at 24 hours (Figure 2*B*). Furthermore, the abundance of exosomes released after irradiation with 4 Gy was time dependent, with a significant increase in exosome abundance at 24 and 48 hours after irradiation and a nonsignificant increase at 12 hours (Figure 2*C*).

Radiation-Derived Exosomes Are Taken Up by Cells in Coculture

Next, we examined whether exosomes derived from irradiated cells influenced their uptake by a recipient cell. Exosomes from nonirradiated cells and irradiated cells (herein referred to as radiation-derived exosomes) were cocultured with U87MG cells and shown to be taken up as early as 30 minutes after their addition (Figure 3*A*). This was quantified by incubating U87MG cells with exosomes at the same concentration for various amounts of time and then analyzing exosome uptake by cells using flow cytometry. This confirmed the confocal observations that uptake of exosomes was time dependent (Figure 3*B*). There was an overall increased uptake of radiation-derived exosomes in recipient cells at 24 hours compared to that of exosomes from nonirradiated cells (Figure 3*C*), which proved to be a significant 1.3-fold increase in uptake (Figure 3*D*). Additionally, U87MG exosomes were taken up by another glioma cell line (U251), as well as normal human astrocytes and HUVECs (Figure W1*C*), showing that exosomes from one cell type could be taken up by cells of different origins.

Radiation-Derived Exosomes Enhance Cell Migration

We recently showed that conditioned media derived from irradiated glioma cells promoted cell migration and invasion [31], and we hypothesized that this effect may be mediated in part by exosome transfer. We tested this with the following two related experiments: 1) by measuring U87MG cell migration when U87MG exosomes were used as a chemoattractant and 2) by measuring migration of U87MG cells that were incubated with U87MG exosomes 24 hours

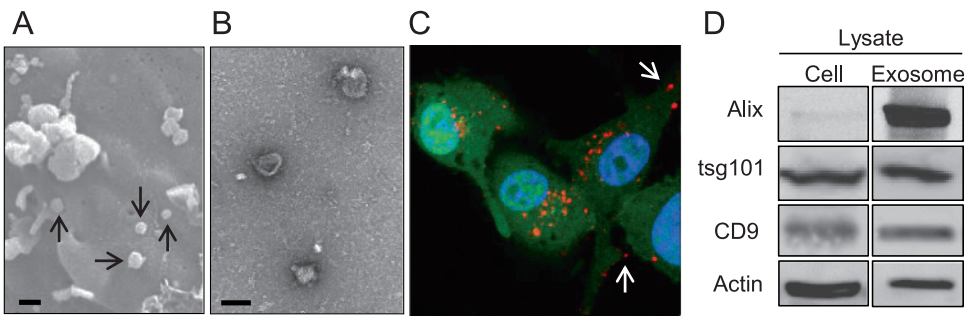

Figure 1. Confirming isolation of exosomes by ultracentrifugation. (A) Scanning electron micrograph of U87MG cell surface with vesicular protrusions (arrows; scale bar, 250 nm) and (B) transmission electron micrograph of purified U87MG exosomes (scale bar, 100 nm). (C) U87MG-GFP cells with PKH26-labeled exosomes in the cytoplasm and on the cell surface (white arrows). (D) Immunoblot analysis shows presence of exosome markers in U87MG exosomes and parent cell line.

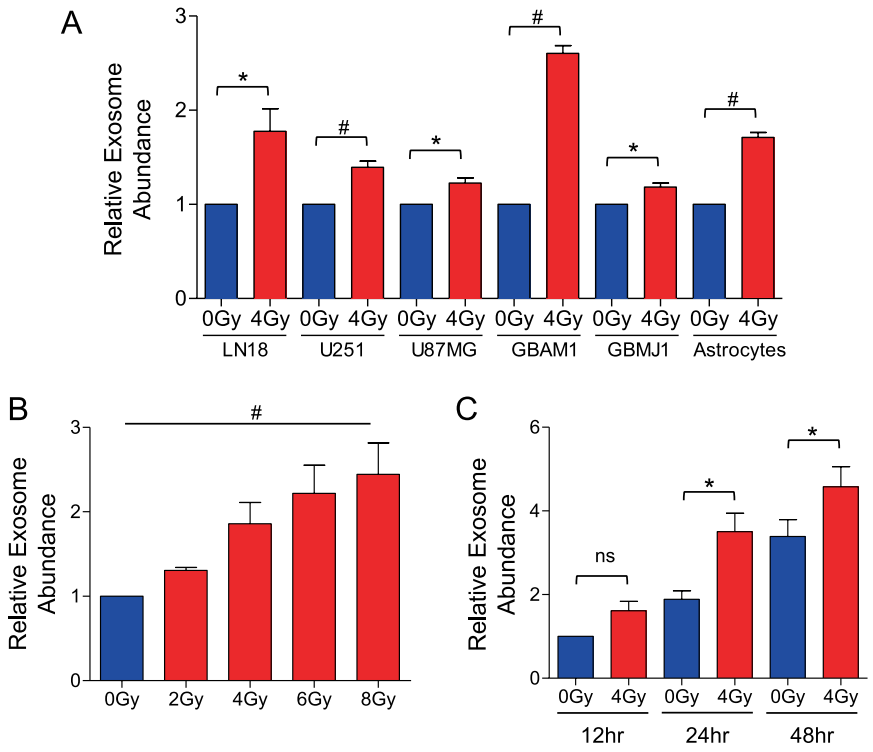

Figure 2. Cellular irradiation increases exosome release. (A) Exosome abundance was measured by NTA at 48 hours after 4-Gy treatment of GBM cells (LN18, U251, and U87MG; $n = 3$), GBM stem-like cells (GBAM1 and GBMJ1; $n = 2$), and normal astrocytes ($n = 3$). (B) U87MG exosomes isolated at 24 hours posttreatment with 2 to 8 Gy were measured by NTA ($n = 3$). (C) Measurement of exosomes released by irradiated (4 Gy) and control cells from 12 to 48 hours after treatment, relative to 0-Gy 12-hour condition ($n = 3$). All graphs represent averaged values relative to 0-Gy condition + SEM; values normalized to number of cells present at time of exosome isolation. $^{*}P < .05$; $^{\#}P < .01$.

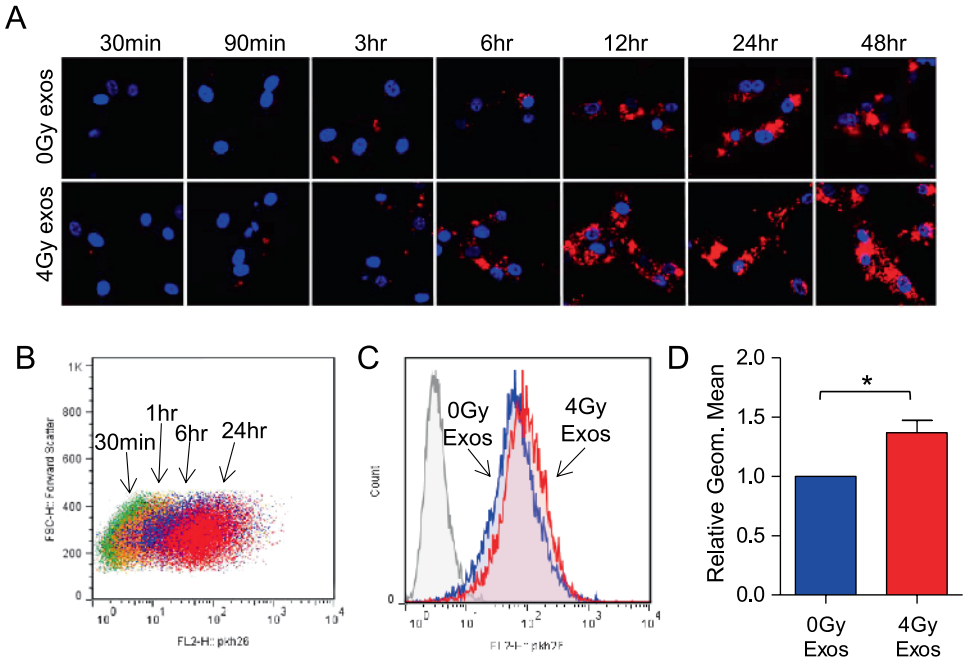

Figure 3. Radiation-derived exosomes are more readily taken up by recipient cells. (A) Confocal microscopic visualization of exosomes within cells. Exosomes are stained red with PKH26, and nuclei are stained blue with DAPI. (B) Flow cytometric quantitation of exosome uptake by cells after 1 to 24 hours in coculture. (C and D) Radiation-derived exosome uptake (4-Gy exosomes) in recipient cells at 24 hours compared with exosomes from nonirradiated cells (0-Gy exosomes) incubated for the same time; (D) is the averaged value + SEM of three independent experiments, relative to the 0-Gy condition. $^{*}P = .03$.

before setting up the assay (Figure 4*A*). In both experiments, exosomes promoted cell migration (Figure 4, *B* and *C*); however, radiation-derived exosomes enhanced this effect, particularly when preincubating exosomes with cells before setting up the assay (Figure 4*C*). The chemotactic effect was influenced by exosome concentration (Figure 4*D*), and radiation-derived exosomes at concentrations ≥25 μg/ml significantly enhanced cell migration compared with exosomes from nonirradiated cells (Figure 4*E*).

To confirm that these effects were indeed the result of the uptake of intact exosomes and not chemical components included with pelleted exosomes (FBS and other chemokines/cytokines), exosomes were lysed with Tx-100 to disrupt vesicle membranes. Tx-100–lysed PKH26-labeled exosomes were no longer taken up in recipient cells (Figure 4*F*), confirming adequate lysis, and no longer induced cell migration (Figure 4*G*); however, dFBS-Tx100 (using the same lysing concentration of Tx-100) and dFBS alone had similar levels of migration, showing that the reduced migration was not due to the presence of Tx-100 in culture conditions. Thus, the uptake of intact exosomes is required to mediate exosome-induced cell migration. Control experiments using the CM and supernatant after pelleting exosomes showed no significant differences between irradiated and unirradiated conditions (Figure W1*D*), which is likely due to the presence of dFBS in all conditions but is removed from exosomes during purification.

Molecular Profiling Reveals Changes Unique to Radiation-Derived Exosomes

Given that radiation-derived exosomes enhanced the migration of U87MG cells *in vitro* compared to exosomes from nonirradiated cells, we characterized molecular drivers contributing to this phenotype.

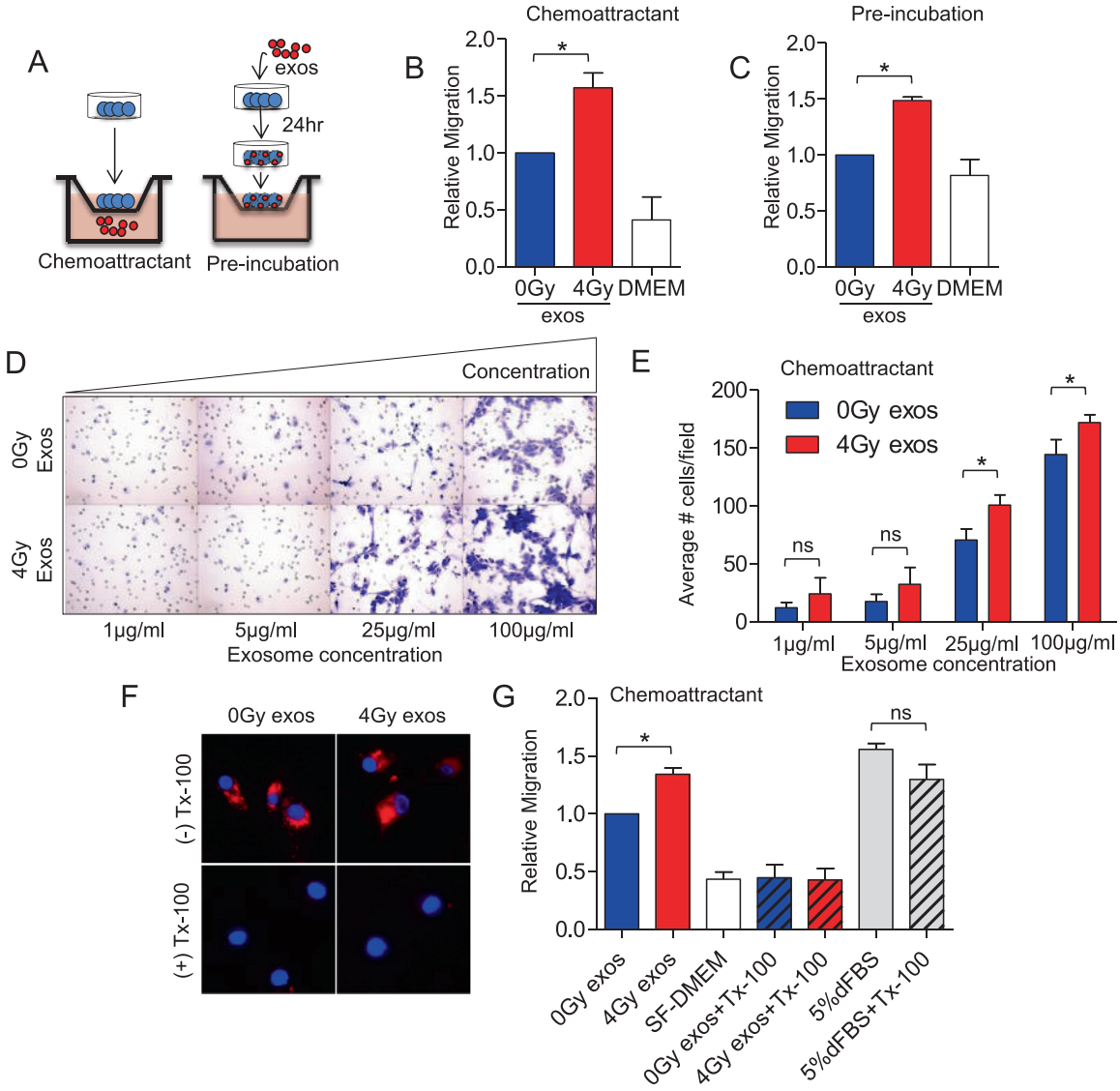

Figure 4. Radiation-derived exosomes enhance cell migration. (A) Schematic of cell migration experiments. (B–E and G) Exosome effect on the migration of U87MG cells across transwell membranes when used as a chemoattractant (B, D, E, and G) or by preincubating exosomes with cells before assay setup (C); $n = 3$. (D) Cell migration in response to increasing exosome concentrations, quantified in E as the averaged values + SEM; $n = 3$. (F) Uptake of PKH26-labeled exosomes before and after Tx-100 lysis. (G) Influence of Tx-100–lysed exosomes and Tx-100/dFBS on cell migration; $n = 3$. Values represent the averaged values + SEM of three independent experiments. Radiation-derived exosomes, 4-Gy exosomes; exosomes from nonirradiated cells, 0-Gy exosomes. *$P < .05$.

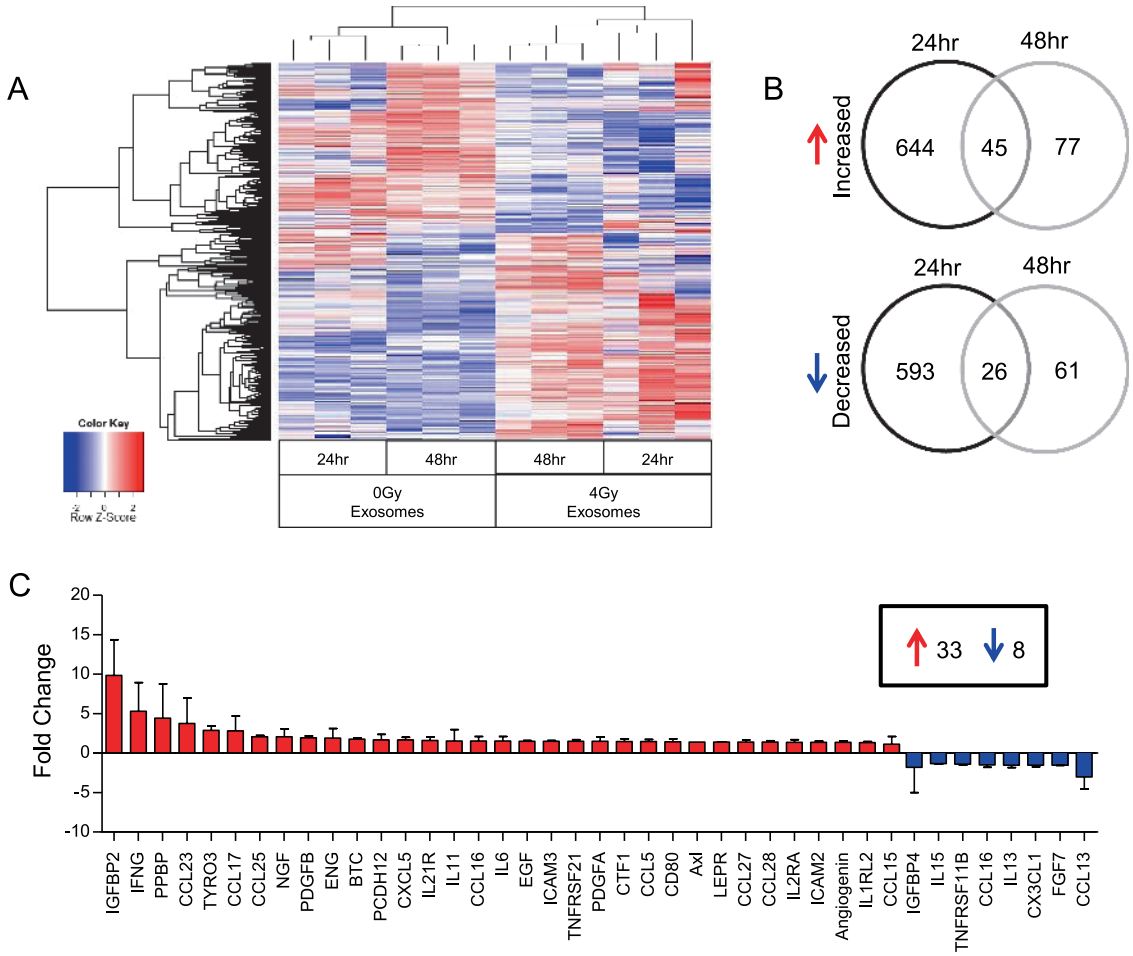

Figure 5. Radiation alters the molecular composition of exosomes. (A) Two-way hierarchical clustering representation of exosome mRNA content. Values shown compare radiation-derived exosomes to those derived from nonirradiated cells at 24 and 48 hours, using a cutoff *P* value of <.05. Up-regulation, red; down-regulation, blue. (B) Venn diagram of the number of significant transcript changes with ≥1.33-fold increased/decreased expression in radiation-derived exosomes compared to exosomes from nonirradiated cells. (C) Protein array analysis of differentially expressed proteins in radiation-derived exosomes compared to exosomes from nonirradiated cells. Values represent those with a ≥1.33-fold increased/decreased expression cutoff comparing radiation-derived exosomes to exosomes from nonirradiated cells ($n = 2$).

Exosomes released by U87MG cells were processed for either total RNA (24 hours and 48 hours postirradiation) or protein extraction (48 hours postirradiation). Two-way hierarchical clustering of cDNA microarray data demonstrated that mRNA changes present in radiation-derived exosomes isolated at 24 and 48 hours (post–cell treatment) were more similar to each other compared with nonirradiated controls (Figure 5*A*). Using a 1.33-fold change cutoff, there were 1308 mRNA changes at 24 hours and 209 mRNA changes at 48 hours in radiation-derived exosomes, with 45 commonly overexpressed and 26 commonly underexpressed transcripts in radiation-derived exosomes at each time point compared to nonirradiated controls (Figure 5*B*). The greater number of mRNA changes at 24 hours compared with at 48 hours may be due to the relatively greater number of exosomes released by U87MG cells after irradiation at 24 hours (Figure 2*B*) compared to the difference at 48 hours (Figure 2*C*). As miRNAs contained in exosomes have demonstrated a functional role on transfer to cells [4], we examined whether cellular irradiation altered the miRNA packaging in exosomes. In contrast to the abundant mRNA changes, radiation-derived exosomes showed few changes in their miRNA composition at both 24 and 48 hours following irradiation (Figure W2, *A* and *B*). Finally, protein microarrays sampling a total of 194 proteins showed 34 proteins with increased abundance and 7 with decreased abundance at 48 hours in radiation-derived exosomes compared to exosomes derived from nonirradiated cells (Figure 5*C*). Overall, molecular profiling showed numerous changes in the contents of radiation-derived exosomes compared to exosomes derived from nonirradiated cells.

Molecular Changes in Radiation-Derived Exosomes Relate to Cell Migration Pathways

IPA was used to categorize the molecular changes in radiation-derived exosomes into functional networks. Exosomes isolated at 48 hours were used in all functional studies to have a sufficient concentration of exosomes for assays, and functional characterization was conducted using molecular changes present at that time point. IPA identified *Cellular Movement* as a top associated network function with a score of 39, as well as the top molecular and cellular function

with 21 molecules and a *P*-value range of .0049 to .00001 (Figure 6*A*). The functional network for *Cell Movement* is shown in Figure 6*B* with the data combined from both the mRNA and protein arrays, with red indicating the upregulated molecules in radiation-derived exosomes. From the pathway in Figure 6*B*, IGFBP2, PDGF-B, chemokine (C-C motif) ligand 23 (CCL23), CCL25 (protein array), CTGF, and Wiskott-Aldrich syndrome protein family member 3 (WASF3; cDNA array) have been implicated in promoting cancer cell migration or invasion [32–37]. The miRNA array data were analyzed separately and showed that the few transcripts that were decreased targeted pathways involved in cell motility (Figure W2*C*); no functional classes were identified for the increased miRNA transcripts. Thus, mRNA and protein array analyses showed similar phenotypic differences in radiation-derived exosomes and further confirmed our observations of their influence on cell migration.

Radiation-Derived Exosomes Enhance FAK Signaling in Recipient Cells On Uptake

Given that radiation-derived exosomes enhanced cell migration and cell movement was a top network on IPA analysis, we investigated known pathways involved in cell migration that could be activated. First, we confirmed a pair of molecules from the molecular profiling that appeared as hubs in the IPA analysis (Figure 6*B*) and were upregulated in radiation-derived exosomes: CTGF from the cDNA arrays and IGFBP2 from the protein arrays. Real-time quantitative PCR confirmed that the CTGF transcript was increased two-fold in radiation-derived exosomes compared with nonirradiated controls (Figure 7*A*, *left*). There was no increase in cellular CTGF mRNA following irradiation (Figure 7*A*, *right*). Immunoblot analysis for CTGF showed no difference in CTGF protein in radiation-derived exosomes (Figure 7*B*, *left*), though an increase was seen in the exosome-secreting cells following irradiation (Figure 7*B*, *right*). There was no change in IGFBP2 mRNA by microarray; however, protein array identified an increase in IGFBP2 protein in radiation-derived exosomes. Immunoblot analysis confirmed that IGFBP2 protein was increased in radiation-derived exosomes (Figure 7*C*, *left*) and in the exosome-secreting cells following irradiation (Figure 7*C*, *right*). These findings suggest that the cellular packaging of exosome content in response to irradiation is selectively altered at the mRNA and protein levels.

Next, we examined how exosomes altered signaling networks in recipient cells on uptake. Immunoblot analysis of cellular lysates 24 hours after exosomes were added in coculture demonstrated that there was an increase in CTGF protein in cells incubated with radiation-derived exosomes (4-Gy exosomes) compared with exosomes from nonirradiated cells (0-Gy exosomes) or those in serum-free medium (DMEM; Figure 7*D*). We confirmed that RNA could be transferred to recipient cells by labeling the RNA in exosomes using a brominated nucleotide (BrUTP; see Materials and Methods section). Coculture of these exosomes (BrUTP exosomes) with nonbrominated cells resulted in the detection of brominated RNA species in the recipient cell (Figure 7*E*, *middle panel*), in a distribution similar to PKH26-labeled exosomes incubated with cells for the same amount of time (Figure 7*E*, *right panel*). This confirmed that RNA packaged into exosomes could be transferred to a recipient cell. In particular, this suggests that the increased abundance of CTGF mRNA in radiation-derived exosomes can be effectively transferred to and translated by a receiving cell into a functional protein with phenotypic modifications.

Of the many pathways involved in cell migration, the FAK signaling cascade plays a role in several cellular processes in response to extracellular stimuli and can be activated by CTGF [33]. Immunoblot analysis revealed that there was activation of members involved in FAK signaling, including TrkA, FAK, Paxillin, and Src by exosomes alone (0-Gy exosomes); however, coculture with radiation-derived exosomes (4-Gy exosomes) further enhanced activation of these signaling molecules (Figure 7*F*). Phosphorylated TrkA and total TrkA levels were increased with exosomes in coculture, and to a greater

A

ID	Associated Network Functions	Score
1	**Cellular Movement**, Carbohydrate Metabolism, Small Molecule Biochemistry	39
2	Cell Morphology, Cellular Function and Maintenance, Drug Metabolism	34
3	Nervous System Development and Function, Tissue Morphology, Developmental Disorder	25
4	Developmental Disorder, Respiratory Disease, Tissue Development	22
5	Cellular Compromise, Cell Death, Renal Necrosis/Cell Death	21

Molecular and Cellular Functions

Name	p-value	# molecules
Cell Movement	1.01E-04 - 4.93E-02	21
Cellular Growth and Proliferation	1.63E-04 - 4.93E-02	20
Cell Signaling	3.24E-04 - 4.93E-02	24
Molecular Transport	7.08E-04 - 4.63E-02	17
Vitamin and Mineral Metabolism	7.08E-04 - 4.63E-02	23

B

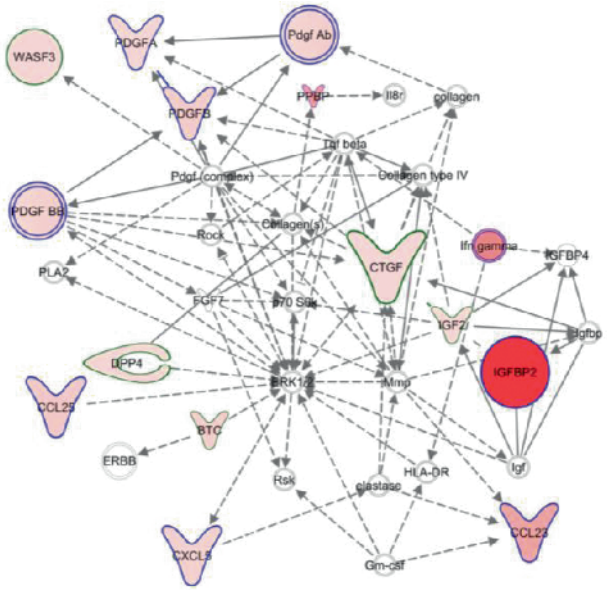

Figure 6. Molecular profile of radiation-derived exosomes relates to pathways involved in cell movement. IPA of top networks from mRNA and protein targets with greater abundance in radiation-derived exosomes. (A) Upper table: *Associated Network Functions*, lower table: *Molecular and Cellular Functions*. (B) Cell movement network is overlaid with values from protein (outlined in blue) and mRNA (outlined in green) arrays using targets with increased abundance in radiation-derived exosomes (red-filled molecules).

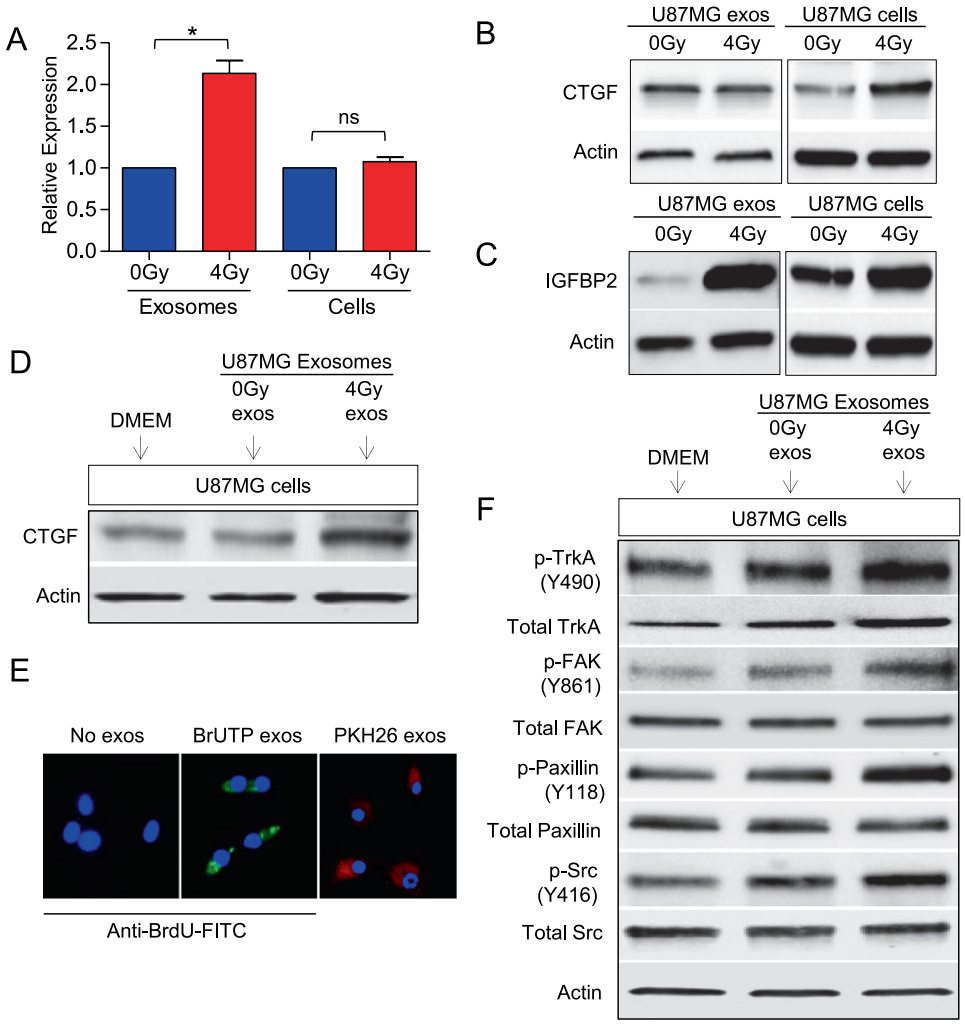

Figure 7. Radiation-derived exosomes augment signaling pathways associated with cell motility. (A) *CTGF* gene expression levels in U87MG exosomes and cells by quantitative reverse transcription–PCR. Data represent averaged values + SEM, $n = 3$; radiation-derived exosomes/cells were compared to nonirradiated controls. $^*P = .0184$. (B) CTGF and (C) IGFBP2 protein levels on immunoblot analysis exosome and whole-cell lysates. (D) Immunoblot analysis of CTGF on lysates from cells incubated for 24 hours in serum-free DMEM or in coculture with exosomes (radiation-derived, 4-Gy exosomes; nonirradiated controls, 0-Gy exosomes). (E) Transfer of BrUTP-labeled mRNA in exosomes to recipient cells (BrUTP exosomes, middle panel). Distribution of PKH26-labeled exosomes incubated for the same time for comparison (right panel). (F) Influence of radiation-derived exosomes and control exosomes on activation of signaling molecules involved in cell migration after coculture with cells for 24 hours.

extent with radiation-derived exosomes, as were phosphorylation levels of FAK, Paxillin, and Src with no change in total protein.

Discussion

Increasing evidence supports exosome transfer as an important mechanism of intercellular signaling in tumors. In particular, this mode of communication has implications for tumor biology, whereby exosomes can transfer biologic factors that alter the phenotype of recipient malignant or stromal cells [7]. Recent work shows that various cellular insults cause tumor cells to increase the release of and alter the molecular composition of tumor exosomes [19,20]. We specifically examine the effect of ionizing radiation on exosome release and signaling and provide evidence that radiation-derived exosomes from GBM cell lines enhance cell migration through a mechanism involving an organized change in exosome mRNA and protein composition (Figure W3).

Our results show that radiation increases exosome release and that this phenomenon is both dose and time dependent. This confirms previous studies reporting this phenomenon [38,39]; however, to our knowledge, this is the first systematic study showing exosome release kinetics using a direct method of exosome measurement by NTA. Although one may argue that dFBS could result in some level of apoptosis due to depletion of factors in the serum, all media growth conditions were identical, and thus, any effect of the media on exosome production was equivalent across all experimental conditions. A recent report noted that p53 status in cells was important for exosome genesis in response to irradiation [38]; however, the current study found that glioma cell lines with mutated p53 (LN18 and U251) appeared to have a greater relative increase in exosome release following irradiation compared with U87, which has wild-type p53. This may be due to the neural origin of the cells studied, whereas Yu et al. [38] examined cell lines of epithelial origin. In addition to studying exosome release, we show that exosomes secreted by a

given tumor line can be taken up by different cell types *in vitro*, including normal astrocytes and endothelial cells. Thus, radiation-mediated exosome release has the potential to affect cells in the tumor microenvironment.

In this study, radiation-derived exosomes were found to enhance cell migration and had a molecular profile containing a greater abundance of mRNA and protein molecules associated with cell motility. Of note, CTGF mRNA and IGFBP2 protein were specifically increased in radiation-derived exosomes, both of which are involved in the migration/invasion of different cancer types, including GBM [32,33,40,41]. CTGF is involved in diverse cellular functions including cell adhesion, migration, survival, and proliferation [40]. We show here that cellular uptake of radiation-derived exosomes increases CTGF protein levels, likely due to translation of transferred exosome mRNA. Edwards et al. demonstrate that CTGF facilitates formation and activation of a CTGF–integrin beta-1 (ITGB1)–TrkA complex, which increases the invasiveness of GBM stem cells [33]. We previously showed that radiation-induced changes in the conditioned media of GBM cells activate members of the FAK signaling cascade and promote GBM cell migration and invasion [31]. FAK signaling involves a diverse set of players involved in its activation and downstream signaling [42]. Activated TrkA interacts with Src [43], whereas Src can directly modulate FAK function and *vice versa* [44,45]. In this study, radiation-derived exosomes enhanced TrkA activation and increase the activation of the following members in the FAK signaling cascade: FAK, Paxillin, and Src, well documented to be involved in cell migration signaling [42,46]. Similarly, IGFBP2 can promote cell migration in various glioma models [32,41,47], and serum protein levels are being investigated as a biomarker for early glioma detection/characterization and predicting prognosis [48,49]. Thus, the molecular changes present in radiation-derived exosomes augment signaling involved in cell migration within the exosome-receiving cell. Other groups have shown that RNA transfer through exosomes can have functional effects on recipient cells [50], and the data here support their work. CTGF signaling through FAK was examined in more detail in light of our previous work, though it is unlikely to be the sole factor influencing the observed phenotype. Signally changes by simple uptake of lipid vesicles, regardless of their content, augment endosomal trafficking and signaling and could explain some of the increased transcriptional/translational activity in recipient cells. This, however, would be similar in both experimental conditions and not explain the enhanced phenotype seen with radiation-derived exosomes. The effect observed is likely a combination of factors—new transcription, translation, and transfer of proteins—that results in the increased migration, and multiple molecules are likely involved. Given that the molecular changes in exosome composition following irradiation were extensive, these are avenues for future work.

In summary, we show that radiation influences the production of exosomes and this effect is dose and time dependent. Radiation-derived exosomes are more readily taken up in coculture with cells and have specific alterations in their molecular composition that enhance cell migration, at least in part due to enhanced activation of TrkA and FAK signaling. Our study sheds light on the influence that therapeutic radiation may have in intercellular signaling through exosomes, and strategies targeting exosomes [51,52] may provide a novel therapeutic approach to counter exosome influence on tumor progression.

Acknowledgments

Thanks to Andrew Byrnes and Gina Conenello (Food and Drug Administration) for assistance with the NanoSight microscope and Mike Kruhlak (National Institutes of Health) for assistance with confocal microscopy. W.T.A. and J.S. received funding as part of the Howard Hughes Medical Institute–National Institutes of Health Research Scholars Program.

References

[1] Camphausen K, Purow B, Sproull M, Scott T, Ozawa T, Deen DF, and Tofilon PJ (2005). Influence of *in vivo* growth on human glioma cell line gene expression: convergent profiles under orthotopic conditions. *Proc Natl Acad Sci USA* **102**, 8287–8292.

[2] Swartz MA, Iida N, Roberts EW, Sangaletti S, Wong MH, Yull FE, Coussens LM, and DeClerck YA (2012). Tumor microenvironment complexity: emerging roles in cancer therapy. *Cancer Res* **72**, 2473–2480.

[3] Lotvall J and Valadi H (2007). Cell to cell signalling via exosomes through esRNA. *Cell Adh Migr* **1**, 156–158.

[4] Al-Nedawi K, Meehan B, Micallef J, Lhotak V, May L, Guha A, and Rak J (2008). Intercellular transfer of the oncogenic receptor EGFRvIII by microvesicles derived from tumour cells. *Nat Cell Biol* **10**, 619–624.

[5] Skog J, Würdinger T, van Rijn S, Meijer DH, Gainche L, Sena-Esteves M, Curry WT Jr, Carter BS, Krichevsky AM, and Breakefield XO (2008). Glioblastoma microvesicles transport RNA and proteins that promote tumour growth and provide diagnostic biomarkers. *Nat Cell Biol* **10**, 1470–1476.

[6] Balaj L, Lessard R, Dai L, Cho YJ, Pomeroy SL, Breakefield XO, and Skog J (2011). Tumour microvesicles contain retrotransposon elements and amplified oncogene sequences. *Nat Commun* **2**, 180.

[7] Lee TH, D'Asti E, Magnus N, Al-Nedawi K, Meehan B, and Rak J (2011). Microvesicles as mediators of intercellular communication in cancer—the emerging science of cellular 'debris'. *Semin Immunopathol* **33**, 455–467.

[8] Rak J (2010). Microparticles in cancer. *Semin Thromb Hemost* **36**, 888–906.

[9] Mineo M, Garfield SH, Taverna S, Flugy A, De Leo G, Alessandro R, and Kohn EC (2012). Exosomes released by K562 chronic myeloid leukemia cells promote angiogenesis in a src-dependent fashion. *Angiogenesis* **15**, 33–45.

[10] Grange C, Tapparo M, Collino F, Vitillo L, Damasco C, Deregibus MC, Tetta C, Bussolati B, and Camussi G (2011). Microvesicles released from human renal cancer stem cells stimulate angiogenesis and formation of lung premetastatic niche. *Cancer Res* **71**, 5346–5356.

[11] Peinado H, Aleèkoviæ M, Lavotshkin S, Matei I, Costa-Silva B, Moreno-Bueno G, Hergueta-Redondo M, Williams C, García-Santos G, Ghajar C, et al. (2012). Melanoma exosomes educate bone marrow progenitor cells toward a pro-metastatic phenotype through MET. *Nat Med* **18**, 883–891.

[12] Putz U, Howitt J, Doan A, Goh CP, Low LH, Silke J, and Tan SS (2012). The tumor suppressor PTEN is exported in exosomes and has phosphatase activity in recipient cells. *Sci Signal* **5**, ra70.

[13] McCready J, Sims JD, Chan D, and Jay DG (2010). Secretion of extracellular hsp90α via exosomes increases cancer cell motility: a role for plasminogen activation. *BMC Cancer* **10**, 294.

[14] Zhang HG, Liu C, Su K, Yu S, Zhang L, Zhang S, Wang J, Cao X, Grizzle W, and Kimberly RP (2006). A membrane form of TNF-α presented by exosomes delays T cell activation-induced cell death. *J Immunol* **176**, 7385–7393.

[15] Taylor DD and Gercel-Taylor C (2008). MicroRNA signatures of tumor-derived exosomes as diagnostic biomarkers of ovarian cancer. *Gynecol Oncol* **110**, 13–21.

[16] Noerholm M, Balaj L, Limperg T, Salehi A, Zhu LD, Hochberg FH, Breakefield XO, Carter BS, and Skog J (2012). RNA expression patterns in serum microvesicles from patients with glioblastoma multiforme and controls. *BMC Cancer* **12**, 22.

[17] Agnihotri S, Burrell KE, Wolf A, Jalali S, Hawkins C, Rutka JT, and Zadeh G (2012). Glioblastoma, a Brief Review of History, Molecular Genetics, Animal Models and Novel Therapeutic Strategies. *Arch Immunol Ther Exp (Warsz)* **1**, 25–41.

[18] Stupp R, Hegi ME, Mason WP, van den Bent MJ, Taphoorn MJ, Janzer RC, Ludwin SK, Allgeier A, Fisher B, Belanger K, et al. (2009). Effects of radiotherapy with concomitant and adjuvant temozolomide *versus* radiotherapy alone on survival in glioblastoma in a randomised phase III study: 5-year analysis of the EORTC-NCIC trial. *Lancet Oncol* **10**, 459–466.

[19] Park JE, Tan HS, Datta A, Lai RC, Zhang H, Meng W, Lim SK, and Sze SK (2010). Hypoxic tumor cell modulates its microenvironment to enhance

angiogenic and metastatic potential by secretion of proteins and exosomes. *Mol Cell Proteomics* **9**, 1085–1099.

[20] King HW, Michael MZ, and Gleadle JM (2012). Hypoxic enhancement of exosome release by breast cancer cells. *BMC Cancer* **12**, 421.

[21] McCord AM, Jamal M, Williams ES, Camphausen K, and Tofilon PJ (2009). $CD133^+$ glioblastoma stem-like cells are radiosensitive with a defective DNA damage response compared with established cell lines. *Clin Cancer Res* **15**, 5145–5153.

[22] Théry C, Amigorena S, Raposo G, and Clayton A (2006). Isolation and characterization of exosomes from cell culture supernatants and biological fluids. *Curr Protoc Cell Biol* **Chapter 3**, Unit 3 22.

[23] Soo CY, Song Y, Zheng Y, Campbell EC, Riches AC, Gunn-Moore F, and Powis SJ (2012). Nanoparticle tracking analysis monitors microvesicle and exosome secretion from immune cells. *Immunology* **136**, 192–197.

[24] Khatua AK, Taylor HE, Hildreth JE, and Popik W (2009). Exosomes packaging APOBEC3G confer human immunodeficiency virus resistance to recipient cells. *J Virol* **83**, 512–521.

[25] Ohtsu M, Kawate M, Fukuoka M, Gunji W, Hanaoka F, Utsugi T, Onoda F, and Murakami Y (2008). Novel DNA microarray system for analysis of nascent mRNAs. *DNA Res* **15**, 241–251.

[26] Goley EM, Anderson SJ, Ménard C, Chuang E, Lü X, Tofilon PJ, and Camphausen K (2004). Microarray analysis in clinical oncology: pre-clinical optimization using needle core biopsies from xenograft tumors. *BMC Cancer* **4**, 20.

[27] György B, Szabó TG, Pásztói M, Pál Z, Misják P, Aradi B, László V, Pállinger E, Pap E, Kittel A, et al. (2011). Membrane vesicles, current state-of-the-art: emerging role of extracellular vesicles. *Cell Mol Life Sci* **68**, 2667–2688.

[28] Camphausen K, Brady KJ, Burgan WE, Cerra MA, Russell JS, Bull EE, and Tofilon PJ (2004). Flavopiridol enhances human tumor cell radiosensitivity and prolongs expression of γH2AX foci. *Mol Cancer Ther* **3**, 409–416.

[29] Camphausen K, Burgan W, Cerra M, Oswald KA, Trepel JB, Lee MJ, and Tofilon PJ (2004). Enhanced radiation-induced cell killing and prolongation of γH2AX foci expression by the histone deacetylase inhibitor MS-275. *Cancer Res* **64**, 316–321.

[30] Mathivanan S and Simpson RJ (2009). ExoCarta: A compendium of exosomal proteins and RNA. *Proteomics* **9**, 4997–5000.

[31] Kil WJ, Tofilon PJ, and Camphausen K (2012). Post-radiation increase in VEGF enhances glioma cell motility *in vitro*. *Radiat Oncol* **7**, 25.

[32] Wang H, Shen W, Huang H, Hu L, Ramdas L, Zhou YH, Liao WS, Fuller GN, and Zhang W (2003). Insulin-like growth factor binding protein 2 enhances glioblastoma invasion by activating invasion-enhancing genes. *Cancer Res* **63**, 4315–4321.

[33] Edwards LA, Woolard K, Son MJ, Li A, Lee J, Ene C, Mantey SA, Maric D, Song H, Belova G, et al. (2011). Effect of brain- and tumor-derived connective tissue growth factor on glioma invasion. *J Natl Cancer Inst* **103**, 1162–1178.

[34] Johnson-Holiday C, Singh R, Johnson E, Singh S, Stockard CR, Grizzle WE, and Lillard JW Jr (2011). CCL25 mediates migration, invasion and matrix metalloproteinase expression by breast cancer cells in a CCR9-dependent fashion. *Int J Oncol* **38**, 1279–1285.

[35] Hwang J, Son KN, Kim CW, Ko J, Na DS, Kwon BS, Gho YS, and Kim J (2005). Human CC chemokine CCL23, a ligand for CCR1, induces endothelial cell migration and promotes angiogenesis. *Cytokine* **30**, 254–263.

[36] Gehmert S, Prantl L, Vykoukal J, Alt E, and Song YH (2010). Breast cancer cells attract the migration of adipose tissue-derived stem cells via the PDGF-BB/PDGFR-β signaling pathway. *Biochem Biophys Res Commun* **398**, 601–605.

[37] Sossey-Alaoui K, Safina A, Li X, Vaughan MM, Hicks DG, Bakin AV, and Cowell JK (2007). Down-regulation of *WAVE3*, a metastasis promoter gene, inhibits invasion and metastasis of breast cancer cells. *Am J Pathol* **170**, 2112–2121.

[38] Yu X, Harris SL, and Levine AJ (2006). The regulation of exosome secretion: a novel function of the p53 protein. *Cancer Res* **66**, 4795–4801.

[39] Lehmann BD, Paine MS, Brooks AM, McCubrey JA, Renegar RH, Wang R, and Terrian DM (2008). Senescence-associated exosome release from human prostate cancer cells. *Cancer Res* **68**, 7864–7871.

[40] Chen CC and Lau LF (2009). Functions and mechanisms of action of CCN matricellular proteins. *Int J Biochem Cell Biol* **41**, 771–783.

[41] Dunlap SM, Celestino J, Wang H, Jiang R, Holland EC, Fuller GN, and Zhang W (2007). Insulin-like growth factor binding protein 2 promotes glioma development and progression. *Proc Natl Acad Sci USA* **104**, 11736–11741.

[42] Hanks SK, Ryzhova L, Shin NY, and Brábek J (2003). Focal adhesion kinase signaling activities and their implications in the control of cell survival and motility. *Front Biosci* **8**, d982–996.

[43] Wooten MW, Vandenplas ML, Seibenhener ML, Geetha T, and Diaz-Meco MT (2001). Nerve growth factor stimulates multisite tyrosine phosphorylation and activation of the atypical protein kinase C's via a src kinase pathway. *Mol Cell Biol* **21**, 8414–8427.

[44] Renshaw MW, Price LS, and Schwartz MA (1999). Focal adhesion kinase mediates the integrin signaling requirement for growth factor activation of MAP kinase. *J Cell Biol* **147**, 611–618.

[45] Sodhi A, Montaner S, and Gutkind JS (2004). Viral hijacking of G-protein-coupled-receptor signalling networks. *Nat Rev Mol Cell Biol* **5**, 998–1012.

[46] Giaccone G and Zucali PA (2008). Src as a potential therapeutic target in non-small-cell lung cancer. *Ann Oncol* **19**, 1219–1223.

[47] Mendes KN, Wang GK, Fuller GN, and Zhang W (2010). JNK mediates insulin-like growth factor binding protein 2/integrin α5-dependent glioma cell migration. *Int J Oncol* **37**, 143–153.

[48] Moore LM, Holmes KM, Smith SM, Wu Y, Tchougounova E, Uhrbom L, Sawaya R, Bruner JM, Fuller GN, and Zhang W (2009). IGFBP2 is a candidate biomarker for *Ink4a-Arf* status and a therapeutic target for high-grade gliomas. *Proc Natl Acad Sci USA* **106**, 16675–16679.

[49] Mehrian-Shai R, Chen CD, Shi T, Horvath S, Nelson SF, Reichardt JK, and Sawyers CL (2007). Insulin growth factor-binding protein 2 is a candidate biomarker for PTEN status and PI3K/Akt pathway activation in glioblastoma and prostate cancer. *Proc Natl Acad Sci USA* **104**, 5563–5568.

[50] Al-Mayah AH, Irons SL, Pink RC, Carter DR, and Kadhim MA (2012). Possible role of exosomes containing RNA in mediating nontargeted effect of ionizing radiation. *Radiat Res* **177**, 539–545.

[51] Al-Nedawi K, Meehan B, Kerbel RS, Allison AC, and Rak J (2009). Endothelial expression of autocrine VEGF upon the uptake of tumor-derived microvesicles containing oncogenic EGFR. *Proc Natl Acad Sci USA* **106**, 3794–3799.

[52] Marleau AM, Chen CS, Joyce JA, and Tullis RH (2012). Exosome removal as a therapeutic adjuvant in cancer. *J Transl Med* **10**, 134.

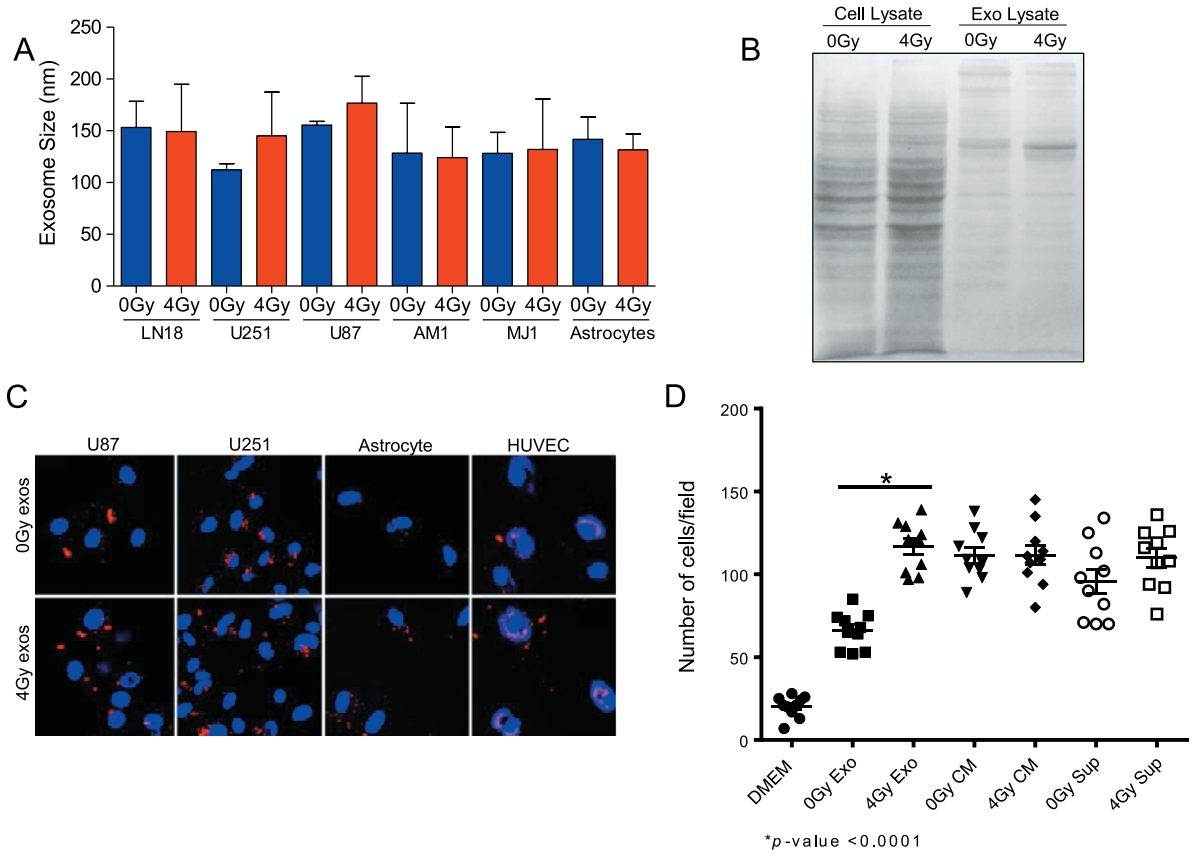

Figure W1. Characteristics of exosomes derived from irradiated cells. (A) Size distribution of exosomes as measured by NTA. Averaged values + SEM (n = 2). (B) Ponceau stain of nitrocellulose membrane containing 30 μg of total U87MG cell and exosome lysates separated by sodium dodecyl sulfate–polyacrylamide gel electrophoresis. (C) Confocal microscopic visualization of U87MG exosome uptake in various GBM cells (U87MG and U251), as well as normal human astrocytes and HUVECs. Exosomes are stained red with PKH26, and nuclei are stained blue with DAPI. (D) Example of U87 cell migration experiment with exosomes, CM, or supernatant after exosome pelleting from irradiated or unirradiated conditions shows only significant changes in exosome-specific experiments. Each point represents an independently counted field.

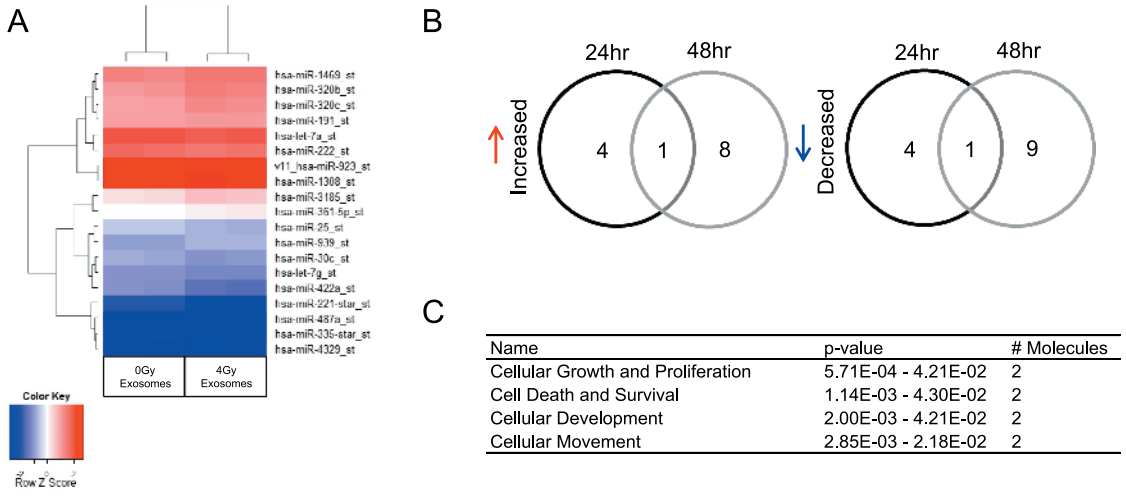

Name	p-value	# Molecules
Cellular Growth and Proliferation	5.71E-04 - 4.21E-02	2
Cell Death and Survival	1.14E-03 - 4.30E-02	2
Cellular Development	2.00E-03 - 4.21E-02	2
Cellular Movement	2.85E-03 - 2.18E-02	2

Figure W2. miRNA profile of exosomes from irradiated and nonirradiated cells. (A) Two-way hierarchical clustering representation of changes in exosome miRNA at 48 hours. Values represent a subset of the data using a P value of $<.05$ comparing radiation-derived exosomes to those from nonirradiated cells at 48 hours. Up-regulation, red; down-regulation, blue. (B) Venn diagram representation of the number of miRNA changes seen in exosomes at 24 and 48 hours following irradiation. (C) IPA of top networks. The miRNA targets that were decreased in exosomes at 48 hours associated with cell movement as one of the top five molecular/cellular functions. No network associations were generated by IPA when the few upregulated miRNA transcripts were used as the input data set.

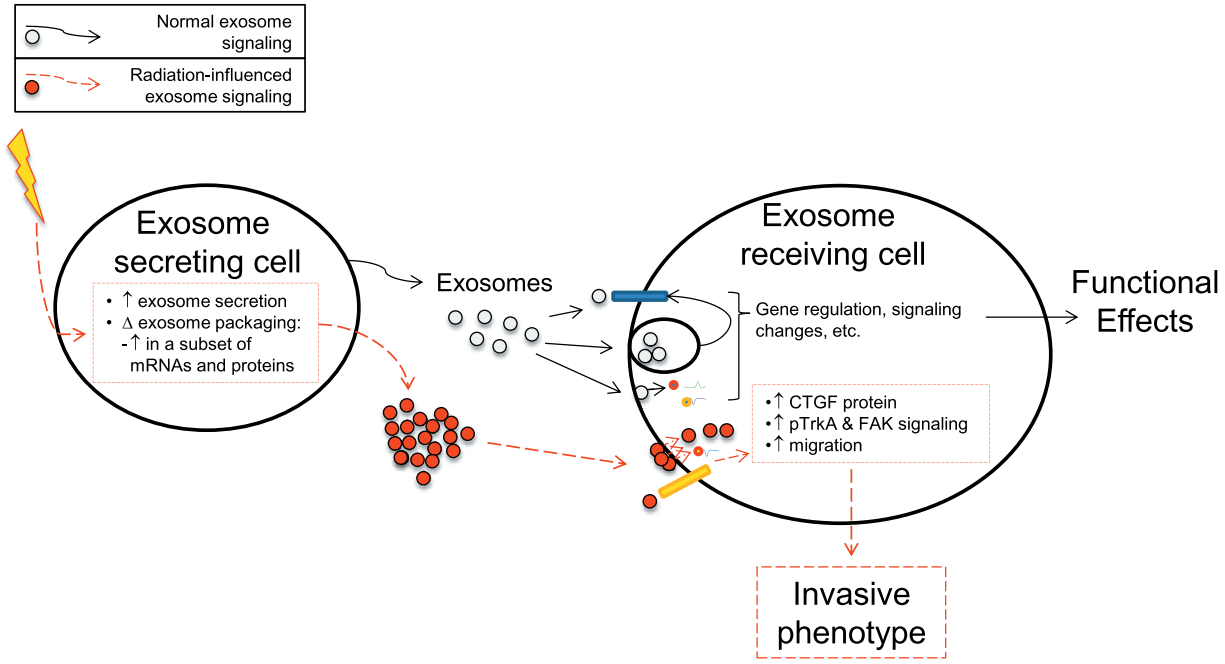

Figure W3. Model of radiation's influence on exosome release and signaling in gliomas. The influence of radiation on exosome release and signaling after uptake in recipient cells is depicted.